ResearchGate

See discussions, stats, and author profiles for this publication at: https://www.researchgate.net/publication/262788652

FT-IR and FT-Raman spectra of 5-fluoroorotic acid with solid state simulation by DFT methods

ARTICLE *in* SPECTROCHIMICA ACTA PART A MOLECULAR AND BIOMOLECULAR SPECTROSCOPY · APRIL 2014

Impact Factor: 2.35 · DOI: 10.1016/j.saa.2014.04.107 · Source: PubMed

READS

104

6 AUTHORS, INCLUDING:

Mauricio Alcolea Palafox

Complutense University of Madrid

129 PUBLICATIONS **1,440** CITATIONS

SEE PROFILE

Vijay Rastogi

Easton Hospital Easton PA 18045

96 PUBLICATIONS **986** CITATIONS

SEE PROFILE

Wolfgang Kiefer

University of Wuerzburg

881 PUBLICATIONS **9,877** CITATIONS

SEE PROFILE

Available from: Mauricio Alcolea Palafox

Retrieved on: 26 January 2016

Spectrochimica Acta Part A: Molecular and Biomolecular Spectroscopy 132 (2014) 430–445

Contents lists available at ScienceDirect

Spectrochimica Acta Part A: Molecular and Biomolecular Spectroscopy

journal homepage: www.elsevier.com/locate/saa

FT-IR and FT-Raman spectra of 5-fluoroorotic acid with solid state simulation by DFT methods

A. Cuellar [a], M. Alcolea Palafox [a,*], V.K. Rastogi [b,c,*], W. Kiefer [d], S. Schlücker [e], S.K. Rathor [c]

[a] Departamento de Química-Física I, Facultad de Ciencias Químicas, Universidad Complutense, Madrid 28040, Spain
[b] R D Foundation Group of Institutions, NH-58, Kadrabad, Modinagar, Ghaziabad, India
[c] Indian Spectroscopy Society, KC 68/1, Old Kavinagar, Ghaziabad 201 002, India
[d] University of Würzburg, Institute for Physical and Theoretical Chemistry, Am Hubland, D-97074 Würzburg, Germany
[e] University of Duisburg-Essen, Faculty of Chemistry, Universitätsstr. 5, D-45141 Essen, Germany

HIGHLIGHTS

- All the tautomers of 5-fluoroorotic acid were described and analyzed.
- The Raman and IR spectra of 5-fluoroorotic acid in the solid state were simulated.
- The solid state simulation was carried out by a dimer and tetramer forms.
- The characteristic skeletal modes in the low wavenumber range were determined.
- The solid state scaled values are in good accordance to the experimental ones.

GRAPHICAL ABSTRACT

Solid state simulation of 5-fluoroorotic acid.

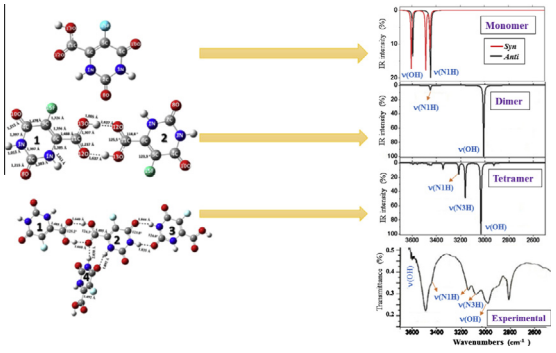

ARTICLE INFO

Article history:
Received 3 February 2014
Received in revised form 11 April 2014
Accepted 22 April 2014
Available online 30 April 2014

Keywords:
5-Fluoroorotic acid
FT-Raman spectroscopy
FT-IR spectroscopy
Vibrational wavenumbers
Tautomerization
Thermodynamic parameters

ABSTRACT

FT-Raman and FT-IR studies of the biomolecule 5-fluoroorotic acid in the solid state were carried out. The unit cell found in the crystal was simulated as a tetramer form by density functional calculations. They were performed to clarify wavenumber assignments of the experimental observed bands in the spectra. Correlations with the molecule of uracil were made, and specific scale equations were employed to scale the wavenumbers of 5-fluoroorotic acid. Good reproduction of the experimental wavenumbers is obtained and the % error is very small in the majority of the bands. This fact confirms our simplified solid state model. The molecular structure was fully optimized using DFT and MP2 methods. The relative stability of both the *syn* and *anti* conformations was investigated, and the *anti*-form was found to be slightly more stable, by 7.49 kJ/mol at the MP2 level. The structures of all possible tautomeric forms were determined. The *keto*-form appeared as the most stable one. The NBO atomic charges and several thermodynamic parameters were also calculated.

© 2014 Elsevier B.V. All rights reserved.

Introduction

Pyrimidines are single ring structures, and the pyrimidine bases are all derivatives of the parent compound pyrimidine. Its derivatives constitute a very important class of compounds because they

* Corresponding authors. Tel.: +34 1913944272.
E-mail addresses: Alcolea@quim.uc.es (M. Alcolea Palafox), v_krastogi@rediffmail.com (V.K. Rastogi).

http://dx.doi.org/10.1016/j.saa.2014.04.107
1386-1425/© 2014 Elsevier B.V. All rights reserved.

are components of the biologically important nucleic acids and have been shown to exert profound physiological effects, and they have been used as antitumor, antibacterial, and antiviral drugs. The orotic acid (uracil-6-carboxylic acid, OA) or vitamin B_{13} and its salts play an important role in biological systems as precursors of pyrimidine nucleoside and are found in cells and body fluids of many living organisms [1a]. 5-Nitroorotic acid, a nitro-derivative of naturally occurring orotic acid (vitamin B_{13}), is a key intermediate in the biosynthesis of the pyrimidine nucleotides of DNA and RNA [1b–d]. These compounds are used in medicine as biostimulators of the ionic exchange processes in organisms. There is also a great interest in the study of orotic acid in relation to food protection and nourishment research [1a]. Orotic acid and its complexes with metal ions have attracted growing attention in medicine: they are used in prophylaxis and treatment of heart diseases and in curing syndromes associated with a deficiency of the essential metal ions [1e].

5-Fluoroorotic acid (5-fluorouracil-6-carboxylic acid, 5-FOA) is a synthetic fluoro derivative of naturally occurring orotic acid (OA). It is a precursor in the novo biosynthesis of series of purines and pyrimidines which has been used in the treatment of certain malignant conditions [2–5]. It induces chromosome alterations [2], and it inhibits the synthesis of mature cytoplasm ribosomal RNA in rat liver cells. It is a noncompetitive inhibitor of dihydroorotase, and it shows antitumor activity against transplanted tumors in rats and mices. It is also a potent inhibitor for some metalloproteins such as dihydroorotase and dihydroorotase dehydrogenase and for thymidylate synthase (nonmetalloprotein) in the human malaria parasite *Plasmodium falciparum* [3,6]. It is incorporated into the ribonucleic acid of animal cells *in vivo,* presumably after decarboxylation to fluorouracil. It has been used too as a selective toxic to yeast cells which synthesize orotidine-5′-phosphate decarboxylase (OMPdecase).

5-FOA is a bactericidal pyrimidine analogue. When it is converted into 5-fluorouridine monophosphate (5-FUMP) it can be incorporated into RNA, as well as further metabolized to 5-fluoro-2′-desoxiuridine monophosphate (5-FdUMP) to act as a potent inhibitor of thymidylate synthase, causing cessation of DNA synthesis. The key enzymes of this pathway are orotate phosphoribosyl transferase (OPRTase) (encoded by pyrE) and orotidine 5′-monophosphate decarboxylase (OMPdecase) (encoded by pyrF). Mutants that lack either of these enzymes are unable to metabolize 5-FOA and hence are resistant to it [7]. 5-FOA can also be considered as a prodrug of 5-fluorouracil (5-FU), which is a potent anticancer and antitumoral drug [3], and has been used against several types of cells [8].

Considering the importance of 5-FOA for medicinal chemistry, however, theoretical studies from the spectroscopy point of view are scarce and in general referred to the calculation of several properties. Also, their vibrational spectra have been relatively little looked into and it has not been completely and rigorously studied yet. Therefore, this is the task undertaken in the present work and as well to make the assignments to different normal modes following the notations of normal modes of the uracil molecule. We have previously analyzed the IR and Raman spectra of 5-aminoorotic acid [9] and several other uracil derivatives [10–12].

Computational methods

The calculations were carried out using MP2 *ab initio* method and Density Functional methods (DFT) [13], including with the Becke's three-parameter exchange functional (B3) [14] in combination with both the correlational functional of Lee, Yang and Parr (LYP) [15]. The B3LYP represents the most cost-effective method [16–19] and therefore it was the only one used in the present manuscript. The B3LYP method was also chosen because different studies have shown that the data obtained with this level of theory were in good agreement than those obtained by other more computational costly methods, such as MP2, and it predicts vibrational wavenumbers of DNA bases better than the HF and MP2 methods [20a], and moreover, it gives the lowest errors in uracil and its derivatives [20b]. All the methods used appear implemented in the GAUSSIAN 03 program package [21]. The UNIX version with standard parameters of this package was running in the alpha computer of the University Complutense of Madrid, Spain.

Several basis sets were utilized starting from the 6-31G(d,p) to 6-311++G(3df,pd). It was noted that 6-31G(d,p) leads to results that represent a compromise between accuracy and computational cost, and for this reason it was the main basis set used in the calculations. The 6-311++G(3df,pd) was utilized for the optimization because it appears close to the energy convergence limit. These basis sets have been previously tested on the uracil molecule [20,22].

The optimum geometry was determined by minimizing the energy with respect to all geometrical parameters without imposing molecular symmetry constraints. Berny optimization under the TIGHT convergence criterion was used. The keyword FREQ was employed for the wavenumber calculations in the harmonic approximation, with the RAMAN option for Raman values. No imaginary wavenumbers appear in the DFT calculated spectra. The natural NBO atomic charges [23] are one of the most accurate today to correlate properties, and they were determined with the keyword POP = NPA.

Experimental

The pure sample of 5-fluoroorotic acid of spectral grade (solid powder) was purchased from Aldrich Chemical Co, USA and used as such without any further purification for recording the FT-IR and FT-Raman spectra. The mid infrared spectrum of the compound in the in the region 400–4000 cm^{-1} was recorded with a Bruker IFS-66 Fourier transform spectrometer equipped with a Globar source, Ge/KBr beamsplitter and a TGS detector at room temperature. For the spectrum acquisition, 50 interferograms were collected at 4 cm^{-1} resolution.

The FT-Raman spectrum in the region 50–4000 cm^{-1} was recorded on a Bruker IFS-66 optical bench with a FRA 106 Raman module attachment interfaced to a microcomputer. The sample was mounted in the sample illuminator using optical mount and no presample pretreatment of any kind was undertaken. The NIR output (1064 nm) of an Nd:YAG laser was used to excite the spectrum. The laser power was set at 250 mW and the spectrum was recorded over 500 scans at a fixed temperature. The spectral resolution was 6.0 cm^{-1} after apodisation.

The full spectra are shown in supplementary material section.

Results and discussion

Geometry optimization in the isolated state

Two possible locations for the carboxylic proton appear in 5-FOA, Fig. 1, according to the value of N1—C6—C11—O13 dihedral angle 0.0° or 180.0°. Thus, two stable conformers were found, designated according to the notation used in OA [1a] as 1 (*syn*) and 2 (*anti*), respectively, Fig. 1. However, we have changed the definition of θ to be the angle N1—C6—C11—O13 ($\theta = 0°$, *syn*) instead of N1—C6—C11═O12 ($\theta = 180°$, *syn*) of Ref. [1a]. The most stable one, conformer 2 is stabilized by a stronger intramolecular interaction through H7 than in conformer 1. This *anti* orientation of the carboxylic group is in accordance to the X-ray data of OA [24].

The difference of energy between both forms is small, 8.68 kJ/mol at B3LYP/6-31G(d,p) level (7.49 kJ/mol at the MP2/6-31G(d,p) level), in agreement with the value of 6.0 kJ/mol reported with the 6-31G(d) basis set in the orotic acid [25], and 6.6 kJ/mol with 6-311G(d,p) [1a]. Calculations carried out by us in OA determine that conformer *anti* is more stable than conformer *syn*. Therefore, we correct the error carried out by the authors [1a] in his Table 4. The energy barrier between both forms is low, 32.05 kJ/mol. However, in 5-FOA the *anti*-form is the only structure expected in the solid state, because its strong intramolecular attraction through H7 blocked its passage to the *syn*-form.

The selected final bond lengths and bond angles optimized in both conformers at the different levels used in the present manuscript are collected in Table 1. These results appear as the most accurate today. The labelling of the atoms is plotted in Fig. 1 and the discussion below is mainly based on the *anti*-form. Crystal structure data have not been reported yet on 5-FOA. Thus, the comparisons were mainly performed with the X-ray data of the orotic acid.

In the data reported on the *anti*-form of OA [25] the carboxylic group appears significantly tilted towards N1-H bond with the C5═C6—C11 angle (124.7°) opener than the N1—C6—C11 angle (113.1°). It is due to the attraction H7···O12 which deforms these angles, with the N1—H7···O of 101.6°. In 5-FOA this difference between C5═C6—C11 and N1—C6—C11 angles, 127.4° and 112.8°, respectively, is higher than in OA. Due to the repulsion O13···F the C5═C6—C11 angle is opened. In the *syn*-form of 5-FOA the difference is lower, 5.6° with the 6-311++G(3df,pd) basis set. It is due to the higher attraction H7···O12 in the *anti*-form than in the *syn* form, which leads to an opening of C5═C6—C11 angle slightly higher in *anti* than in *syn*-form. The small *tilt* towards N1—H of the carboxylic group also leads to a decrease in the asymmetry of the C6—C11═O12 and C6—C11—O13 angles: 121.4° and 114.3°, respectively in the *anti*-form, and 125.7° and 110.6° in the *syn*.

Compared to uracil (U) several general features due to the —F and —COOH substituents are observed in the *anti*-form of 5-FOA at the B3LYP/6-311++G(3df,pd) level:

(i) The substituent F withdraws negative charge on C5, which passes to a positive value, and consequently a lengthening of the C4—C5 and C5═C6 bonds is produced. Thus, the C4—C5 bond is 1.455 Å in (U) vs. 1.472 Å in 5-FOA.
(ii) The N3—C4 bond length is shortened, 1.408 Å in (U) vs. 1.392 Å in 5-FOA, as well as C2═O (1.210 Å in (U) vs. 1.208 Å), while in C4═O is slightly lengthened (1.213 Å in (U) vs. 1.228 Å) as well as N1—C6. However, in OA the N1—C6 bond length is shorter than in 5-FOA.
(iii) The N3—H bond length is little influenced by —F or —COOH substituents, while the N1—H bond appears slightly shortened in 5-FU [26], and slightly lengthened by —COOH in 5-FOA due to an intramolecular H-contact.
(iv) The substituents —F and —COOH also affect the ring angles with a reverse effect, an opening of the *ipso* C4-C5═C6 angle (119.8° in (U) vs. 121.1° in 5-FOA) and a closing of N1—C6═C5 (122.0° vs. 119.7°). These features also produce a slight closing of N3—C4—C5 and an opening of C2—N1—C6 angles. The mutual stearic interaction of both substituents also contributes to the deformation of these surrounding angles. As expected, the C2—N3—C4 and N1—C2—N3 angles remain almost unchanged.

Tautomerism

The nucleic acid bases can undergo *keto–enol* tautomerism. This feature is common to all pyrimidines [12d]. Much of the interest in the tautomerism is due to the fact that tautomers induce alterations in the normal base pairing, leading to the possibility of spontaneous mutations in the DNA or RNA helices. Tautomerism in nucleic acid bases has a role in mutagenesis of DNA. The process is intimately connected with the energetic of the chemical bonds. The tautomerization process involves a 1,3-proton shift, where a proton is transferred from the nitrogen atom to the more electronegative oxygen atom. The tautomerism of orotic acid have been studied at the B3LYP/6-311G(d,p) level by Hilal et al. [1a], in which four *enol* forms are described as well as a zwitterion form. However, to the best of our knowledge, the tautomerism on 5-FOA has not been reported yet. Therefore, we have also included a study of its tautomerism in the present manuscript.

5-FOA can exist in various tautomeric forms differing from each other by the position of the proton, which may be bound to either nitrogen or oxygen ring atoms. Proton migration causes expected sizeable variations in the ring structure and the exocyclic CO bond lengths. Of all the possible combinations, the 10 *enol* tautomers plotted in Fig. 2 are the most stable ones. This figure shows the optimized structures with the notation used. The gas-phase relative energies are shown in Table 2, which can be compared with those corresponding to (U) molecule. The notation used for the tautomers of uracil molecule is that used in the bibliography [20,22]. Unfortunately there are not studies of 5-FOA to compare our results, but the accordance found in our calculated data of uracil molecule using the B3LYP method with those reported by other authors, experimentally and theoretically, permit us to assume that the calculated values shown in Table 2 are satisfactory and they are the only data reported today.

As in uracil molecule, in the isolated state the keto form **T1** of 5-FOA is the most stable one. The next most stable tautomer is the *enol* form **T2a**, and a very close tautomer **T3a**. Their relative

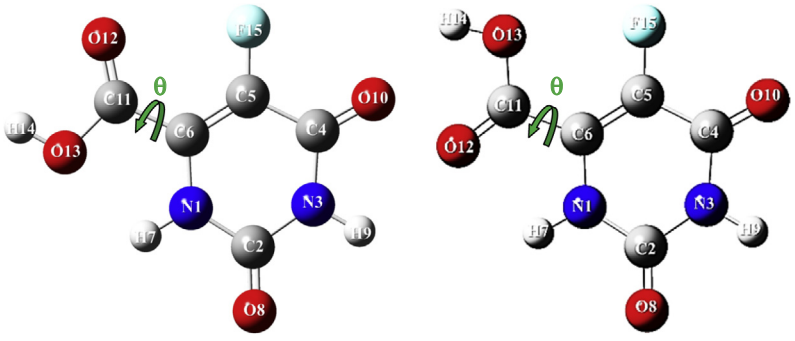

Conformer 1 (θ=0º, *Syn*) **Conformer 2 (θ=180º, *Anti*)**

Fig. 1. Labeling of the atoms in the *syn* and *anti*-conformations of the isolated state of 5-FOA by rotation of the θ (N1—C6—C11—O13) torsional angle.

Table 1
Geometrical parameters, bond lengths (in Å) and angles (in degrees) calculated with B3LYP and MP2 methods and different basis set in the two conformers of 5-FOA.

Parameters	Conformer 1 (*syn*)			Conformer 2 (*anti*)		
	B3LYP/6-31G(d,p)	B3LYP/6-311++G(3df,pd)	MP2/6-31G(d,p)	B3LYP/6-31G(d,p)	B3LYP/6-311++G(3df,pd)	MP2/6-31G(d,p)
Bond lengths						
N1—C2	1.384	1.379	1.381	1.382	1.377	1.379
C2—N3	1.394	1.388	1.394	1.396	1.390	1.396
N3—C4	1.398	1.393	1.395	1.397	1.392	1.394
C4—C5	1.474	1.472	1.468	1.474	1.472	1.469
C5=C6	1.356	1.351	1.360	1.355	1.349	1.359
N1—C6	1.388	1.384	1.385	1.384	1.380	1.382
N1—H7	1.010	1.009	1.009	1.013	1.012	1.011
N3—H9	1.013	1.012	1.012	1.013	1.012	1.012
C2=O	1.215	1.208	1.222	1.214	1.208	1.221
C4=O	1.215	1.207	1.224	1.216	1.228	1.225
C5—F	1.325	1.317	1.333	1.328	1.321	1.335
C6—C11	1.489	1.490	1.485	1.490	1.491	1.485
C11=O12	1.206	1.196	1.215	1.215	1.205	1.223
C11—O13	1.358	1.355	1.362	1.338	1.333	1.342
O13—H14	0.971	0.969	0.971	0.972	0.970	0.972
Bond angles						
N1—C2—N3	112.9	113.2	112.5	112.7	113.0	112.3
C2—N3—C4	128.4	128.1	129.0	128.5	128.2	129.0
N3—C4—C5	112.8	112.9	112.4	112.7	112.9	112.4
C4—C5=C6	121.4	121.3	121.5	121.1	121.1	121.2
N1—C6=C5	119.4	119.4	119.4	119.8	119.7	119.6
C2—N1—C6	124.9	124.8	124.9	124.9	124.9	125.1
N1—C2=O8	123.5	123.4	123.8	123.8	123.7	124.2
N3—C4=O10	122.7	122.4	122.8	122.7	122.6	122.9
C4—C5—F	115.6	115.6	115.8	115.6	115.5	115.8
C6=C5—F	122.9	123.0	122.5	123.1	123.2	122.9
C5=C6—C11	122.9	123.1	122.9	127.4	127.4	127.5
C6—C11=O12	125.6	125.6	125.8	127.4	121.4	121.5
C6—C11—O13	110.6	110.7	110.1	114.1	114.3	113.6
O12=C—O13	123.6	123.6	124.0	124.3	124.3	124.7
N1—C6—C11	117.5	117.5	117.6	112.7	112.8	112.8

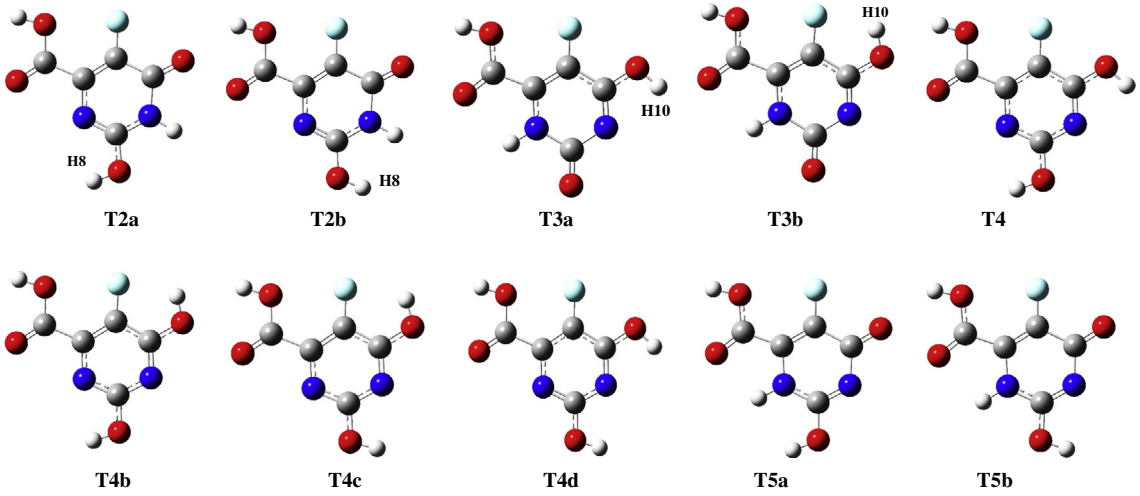

Fig. 2. Optimum structure of the enol tautomers in conformer 2 of 5-FOA.

energies are ca. 8.37 kJ/mol less stable than tautomer U2 of uracil molecule, Table 2. The remaining *enol* tautomers appear less stable than those corresponding to U molecule. This lower stability of the *enol* tautomers of 5-FOA as compared to U may be because of the attraction H7···O12 which makes difficult the H-bond of H7 with O8 in tautomers **T2a** and **T4**. In **T3a** the lower negative charge on O10 in 5-FOA than in U makes difficult the H-bonding of H9 to O10. i.e. the stability of **T3a** is lower in 5-FOA than in U. The stability of the *enols* tautomers considering the thermal correction to the energy, ΔG, is slightly higher than considering ΔE. The calculations with the 6-311++G(3df,pd) basis set give rises to similar stability, but with slightly lower ΔE values, less than 4 kJ/mol.

The —COOH group leads to a slightly lower negative charge on N1 and O8 atoms as compared to that of uracil, and a decrement in the negative charge on O8 has been related [27] to a decrease in the stability of tautomer **T2.** The negative charge on N3 and O10 atoms in 5-FOA is also lower as compared to that of uracil, i.e. all the tautomers in 5-FOA are less stable than in uracil.

The effect of the fluorine atom was observed in 5-fluorouracil, with a reduction of about 8% in the relative energies of the two most stable *enol* tautomers, **T2** and **T4** [27]. However, this effect is smaller as compared to that of the carboxylic group, and thus the tautomerism in less favored in 5-FOA than in U.

Table 2
Gas-phase relative energies (kJ/mol) of uracil and 5-FOA tautomers with the B3LYP DFT method.

5-FOA					Uracil	
Tautomer	6-31G(d,p)		6-311++G(3df,pd)		6-311++G(3df,pd)	
	ΔE + ZPE	ΔG	ΔE + ZPE	ΔG	Tautomer	ΔE + ZPE
T1 (ceto)	0[a]	0[b]	0[c]	0[d]	U1	0
T2a	55.2	52.7	53.9	55.6	U2	46.5
T2b	91.1	86.9	84.4	82.3		
T3a	55.6	55.6	53.9	53.9	U3	48.2
T3b	71.5	71.5	68.6	70.6		
T4	67.3	63.1	64.4	63.5	U4	53.9
T4b	76.5	74.0	74.4	76.5		
T4c	79.8	78.2	75.7	74.8		
T4d	74.8	73.6				
T5a	101.6	100.7	94.9	96.1		
T5b	65.2	65.2			U5	79.0

[a] −702.522408 A.U.
[b] −702.558376 A.U.
[c] −702.786012 A.U.
[d] −702.822069 A.U.

The attractive effect of the fluorine atom on the H10 hydroxyl hydrogen atom produces a slight closing of the C4—C5—F angle, 117.6° in **T3b** vs. 119.3° in **T3a**, and an opening of the C—C5=C angle, 118.1° vs. 116.8°, respectively. The carbonyl oxygen O10 also gives rises to a closening of the C4—C5—F angle as compared to an OH group, 114.2° in **T2a** vs. 119.3° in **T3a**, and the corresponding opening of the C—C5=C angle, 121.7° vs. 116.8°, respectively.

The —COOH moiety appears in the plane of the uracil ring. The exception is observed in tautomers **T2b, T4, T4c** and **T4d** with a rotated —COOH group. Thus, in **T4d** the N1—C6—C=O torsional angle is 22.9° with the 6-31G(d,p) basis set. The planar form is a first order saddle point. The difference of energy between both forms is very small, 0.10 kJ/mol. Small rotations are observed in **T4c** (17.1°), **T2b** (8.7°) and **T4** (4.9°) with the 6-31G(d,p) basis set. However, the rotation increases remarkably with the 6-311++G(3df,pd) basis set, e.g. **T4c** (40.3°), **T2b** (39.7°) and **T4** (36.5°).

Dimer and tetramer simulation of the crystal structure

According to the X-ray crystal data of carboxylic acid derivatives and of orotic acid, the molecules of 5-FOA are expected to be associated in the crystal structure to form ribbons stabilized by N—H···O and O—H···O hydrogen bonds which involve the NH and OH groups and the carbonyl oxygen atom of C=O groups. As a simplification of this system, we have considered only 2 and 4 molecules of the unit cell, the dimer (Fig. 3) and tetramer (Fig. 4) forms, respectively, for the simulation of the solid state. The proposed structure for the tetramer is based in the X-ray data of orotic acid. The most important calculated geometrical parameters are included in these figures.

With the *anti* form the dimer of Fig. 3 was simulated at the B3LYP/6-31G(d,p) level. A slight lengthening of the C11=O bond length of 0.022 Å and of C11—O13 of 0.031 Å is observed in the dimer formation. As consequence, the OCO angle is slightly opened, 1.2°. The C6—C11 and the C—F bond lengths remain almost unchanged, with a very small shortening in the dimer form, 0.002 Å. The fluorine atom has no influence in the dimer formation, and thus both H-bonds have the same length.

The tetramer structure appears stabilized by strong H-bonds through the C=O and N—H bonds that leads to a planar form with the molecules 1–3, Fig. 4b. Also these H-bonds give rise to a lengthening of the C2=O, and C4=O bonds and consequently, the neighboring N3—C4 and C4—C5 bonds appear shortened ca. 0.02 and 0.004 Å respectively. The N3—H···O=C2 H-bond is slightly stronger than N3—H···O=C4 in accordance to a higher negative charge on O8 atom than on O10 atom. 4th molecule is out-of-plane due to the repulsion of its O8 atom with the oxygen O13 of molecule 1. As consequence of this repulsion the N3—H(molecule 4)···O12(molecule 2) H-bond is something long, 2.030 Å. In the crystal, the packing forces are expected to reduce/eliminate this non-planarity of molecule 4, with a noticeable lengthening of the N3—H(molecule 4)···O12(molecule 2) and N1—H(molecule 2)···O10(molecule 4) H-bonds.

The strongest H-bonds correspond to those with the carboxyl moiety. In the dimer both H-bonds have the same stretch, but in the tetramer form differs slightly due to the H-bond with molecule 4.

Due to the orientation of the N1—H and —COOH groups in molecules 3 and 4 of our tetramer simulation, they do not have interaction with other molecules, and thus their calculated bond lengths and angles are the same as that in the isolated state. Thus, differences are expected in them in the crystal with longer C=O and N—H bond lengths. The H-bonds through N1—H and COOH groups in molecules 1 and 3, respectively, with the neighboring molecules could stabilize the tetramer form.

Although X-ray data of this molecule are not available, however, our simulated IR and Raman spectra of this tetramer form are in good accordance to the experimental ones in the solid state. Therefore, it is expected that this tetrameric form of 5-FOA appears in the crystal, but with the ring 4 in the plane of the other rings, due to the packing forces of the crystal.

Calculated atomic charges

The values of the natural charges obtained are listed in Table 3. For simplicity, and also because the small differences observed between conformers 1 and 2, only the results calculated in conformer 2 are shown in the present manuscript. As NBO charges

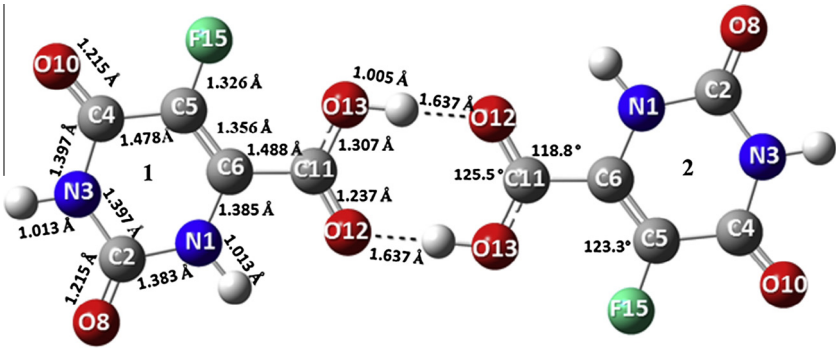

Fig. 3. Labeling of the atoms in the dimer form of 5-FOA.

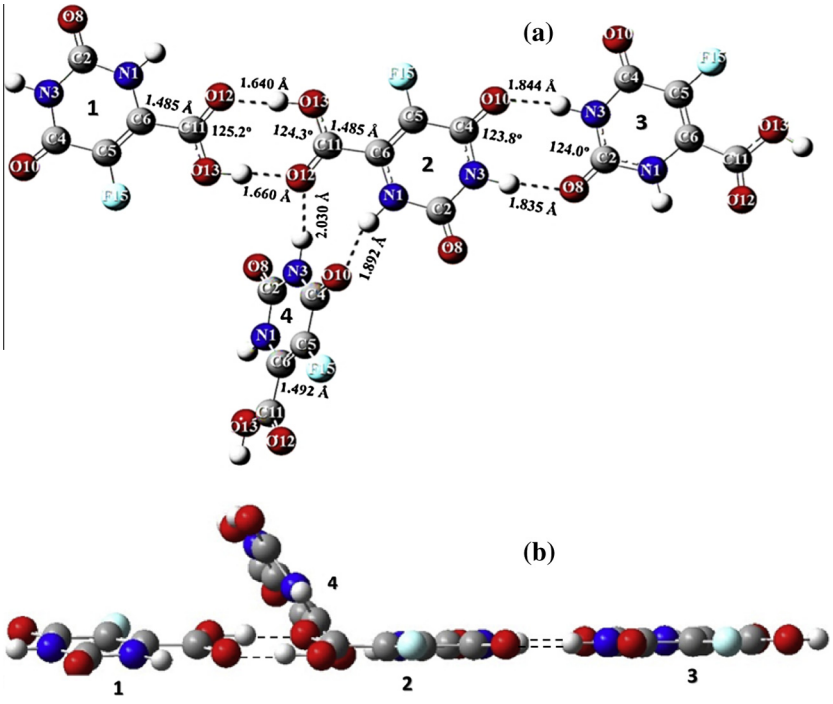

Fig. 4. Simulation of the solid state: two views, (a) and (b), of the optimized tetramer form of 5-FOA at the B3LYP/6-31G(d,p) level.

appear very reliable, therefore, they are the only ones studied in detail in the present study. For comparison purposes, the NBO charges calculated in (U) molecule are also included in Table 3. It is interesting to observe in 5-FOA the effect of electron withdrawing (—F) substituent and the (—COOH) group on the uracil ring. The main features observed in 5-FOA related to (U) are as follows:

Because of substituents a strong change in the charges on C5 and C6 atoms is observed. The effect due to the substituent —F on the uracil ring is higher than due to the —COOH substituent. The negative charge on C5 atom is much more reduced (it passes to a positive value) than the decrease in positive charge on C6 atom. The same effect of the fluorine atom was also observed in 5-fluorouracil molecule [27]. However, the calculated value of the charge on C6 atom is similar to that as obtained in orotic acid.

(i) The negative charge on the fluorine atom in 5-FOA is slightly less negative than on the fluorine atom in 5-FU [27]. This negative charge on the fluorine atom in 5-FOA leads to a slight decrease of the negative charge on the O8 and O10 atoms, and as well as on N3 atom.

(ii) The negative charge on N1 atom is slightly reduced, and consequently the value of the positive charge on H7 atom is increased. In this increment of charge on H7 atom a slight contribution is also due to the interaction with the carbonyl oxygen atom O12. Also, the negative charge on N1 atom is lower than on N3 atom, but the N1—H bond length (1.012 Å) is the same as that of the N3—H bond, 1.012 Å, in contrast to that observed in (U), with a larger N1—H bond than N3—H. Thus, in 5-FOA the acidity of the N1—H bond is higher than the N3—H bond.

(iii) The negative charge on O10 atom is noticeably reduced to 0.040*e* at the MP2 level, where *e* is the charge of the electron, and as consequence, the positive charge on C4 atom is also reduced by similar amount, 0.052*e*. It is because of the strong effect of substituent F on C5 atom. O8 atom is also affected by the substituents, with a small reduction in its negative value.

(iv) The negative charge on O8 atom is larger than on O10 atom, and the C2═O bond is slightly shorter than the C4═O bond, i.e., the basicity of the O8 atom is higher than that of the O10 atom. This fact is in accordance to that already observed in (U) molecule [20,22].

Vibrational wavenumbers

The FT-IR and Raman spectra of 5-FOA are shown in good quality in Fig. 1-Sup–Fig. 3-Sup (Supplementary Material). The study is divided into two regions: 3700–2500 cm^{-1} (Figs. 5 and 6) and

Table 3
Calculated natural NBO atomic charges in uracil and in conformer 2 of 5-FOA with the B3LYP and MP2 methods.

Atom	B3LYP/6-311++G(3df,pd)		MP2/6-31G(d,p)		Atom	B3LYP/6-311++G(3df,pd)	MP2/6-31G(d,p)
	Uracil	5-FOA	Uracil	5-FOA		5-FOA	
N1	−0.610	−0.598	−0.738	−0.729	C11	0.794	0.973
C2	0.822	0.822	1.014	1.015	O12	−0.596	−0.690
N3	−0.642	−0.634	−0.784	−0.779	O13	−0.656	−0.758
C4	0.654	0.613	0.819	0.767	H14	0.496	0.536
C5	−0.359	0.346	−0.451	0.376	F15	−0.300	−0.351
C6	0.081	0.030	0.119	0.042			
H7	0.417	0.442	0.462	0.488			
O8	−0.630	−0.618	−0.730	−0.717			
H9	0.421	0.424	0.467	0.475			
O10	−0.600	−0.567	−0.694	−0.654			

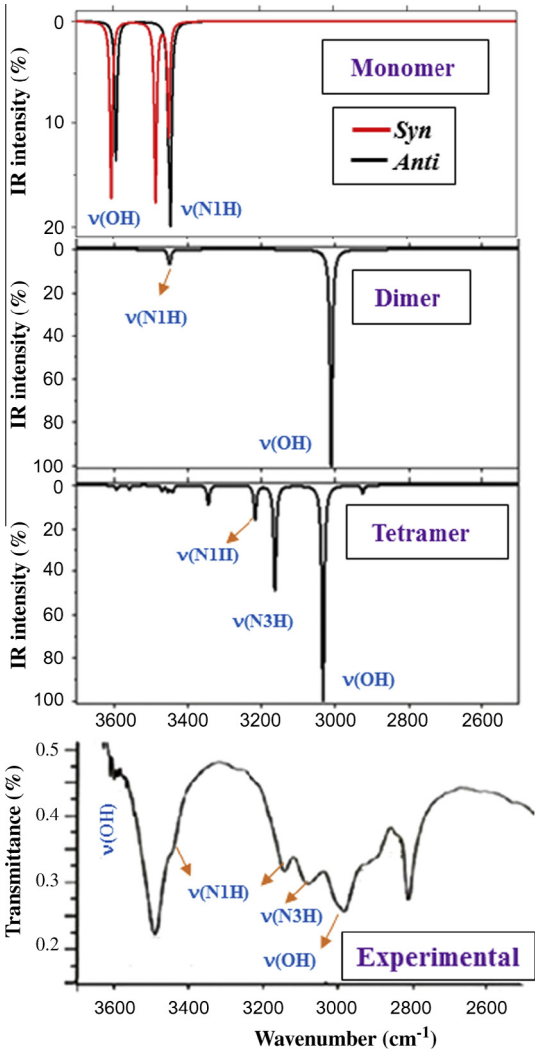

Fig. 5. Theoretical scaled IR spectrum in the 3700–2500 cm^{-1} range of 5-FOA using the scale equation procedure in the monomer, dimer and tetramer simulations, and comparison with the experimental ones.

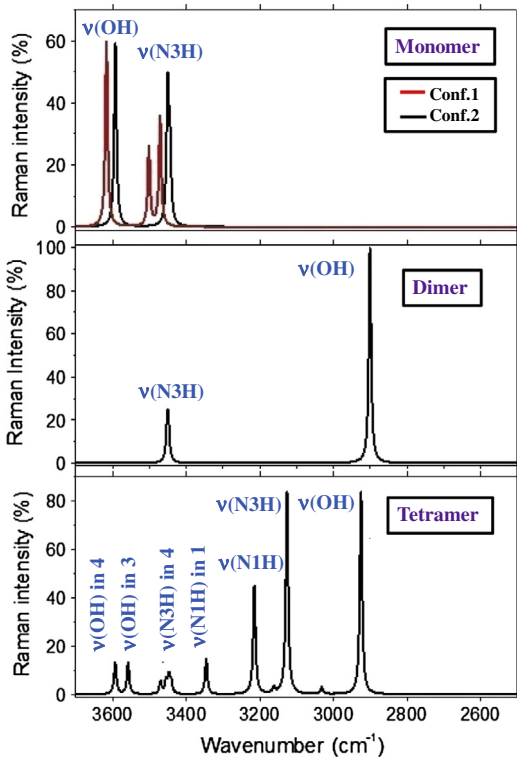

Fig. 6. Theoretical scaled Raman spectrum in the 3700–2500 cm^{-1} range of 5-FOA using the scale equation procedure in the monomer, dimer and tetramer simulations.

2000–400 cm^{-1} (Figs. 7 and 8). In these figures the scaled IR and Raman spectra of 5-FOA were simulated using the scaling equation procedure [22] and they were compared with the experimental FTIR and FT-Raman spectra. The harmonic vibrational bands computed in the isolated state and in the dimer and tetramer forms are collected in Tables 4 and 6, while the scaled ones are listed in Tables 5 and 7.

Scaling the wavenumbers

In Table 5 appears the scaled wavenumbers in 5-FOA obtained by one of the best procedures of scaling [16–18,28,29], i.e. by using a scale equation. With this procedure of scaling, the error obtained in the scaled wavenumbers is in general lower than 5%, which permits an accurate correlation with the experimental bands and thus their assignments. This procedure of scaling requires the previously calculated wavenumbers of the uracil molecule [22] determined at the same computational level. Thus, the scaling equations required for the uracil ring modes in 5-FOA are: $\nu_{scaled} = 31.9 + 0.9512 \cdot \omega_{calculated}$ with the 6-311+G(3df,pd) basis set, and $\nu_{scaled} = 34.6 + 0.9447 \cdot \omega_{calculated}$ with the 6-31G(d,p). For the carboxylic group is used the scaling equation determined in benzoic acid [30]: $\nu_{scaled} = 18.8 + 0.9462 \cdot \omega_{calculated}$. For comparison purposes, the scaled wavenumbers and the IR experimental values in gas phase determined in uracil molecule are also shown in the 1st and 2nd columns, respectively.

The scaling equation procedure, developed by one of the authors, represents a compromise between accuracy and simplicity over other procedures of scaling, and therefore, it was the only one used for scaling the wavenumbers, Figs. 5–8. The scaled dimer and tetramer values, 5th and 6th columns of Table 5, respectively, can be compared with the experimental IR and Raman data, columns 7th–8th. With the scaled values a close agreement with the experimental data was obtained in the majority of the cases with low absolute errors, column 8th, as compared to those with calculated wavenumbers, column 7th. These values are very close to those obtained in related molecules earlier studied by us [18,19,31]. However, large differences are observed in the groups involved in H-bonds, especially in the stretching region.

Vibrational modes

For the study of the vibrational bands, the discussion appears divided in two main sections, the uracil ring modes and the carboxylic group modes. Because the tetramer form represents a better simulation of the solid state as compared to dimer, the discussion of the vibrational bands is mainly based on this tetramer form. Clear differences between both forms are observed in the bands corresponding to the C2═O, C4═O, N1—H and N3—H groups of 5-FOA, because they are not involved in H-bonds in the dimer, but they appear H-bonded in some molecules of the tetramer.

Uracil ring vibrations

The third column of Table 4 lists for conformer 2 the calculated wavenumbers (in cm^{-1}) in increasing order with their relative (in %) infrared (*A*) and Raman (*S*) intensities, fourth–fifth columns,

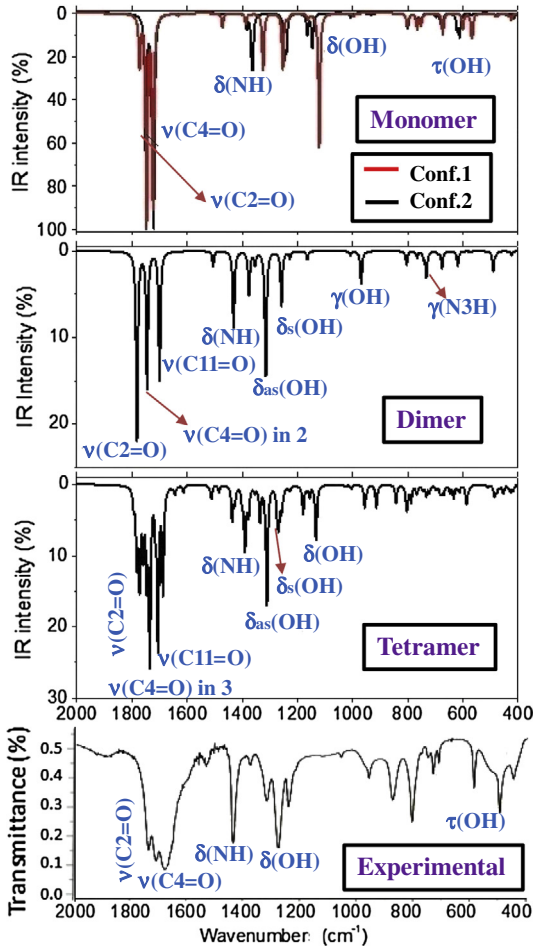

Fig. 7. Theoretical scaled IR spectrum in the 2000–400 cm^{-1} range of 5-FOA using the scale equation procedure in the monomer, dimer and tetramer simulations, and comparison with the experimental ones.

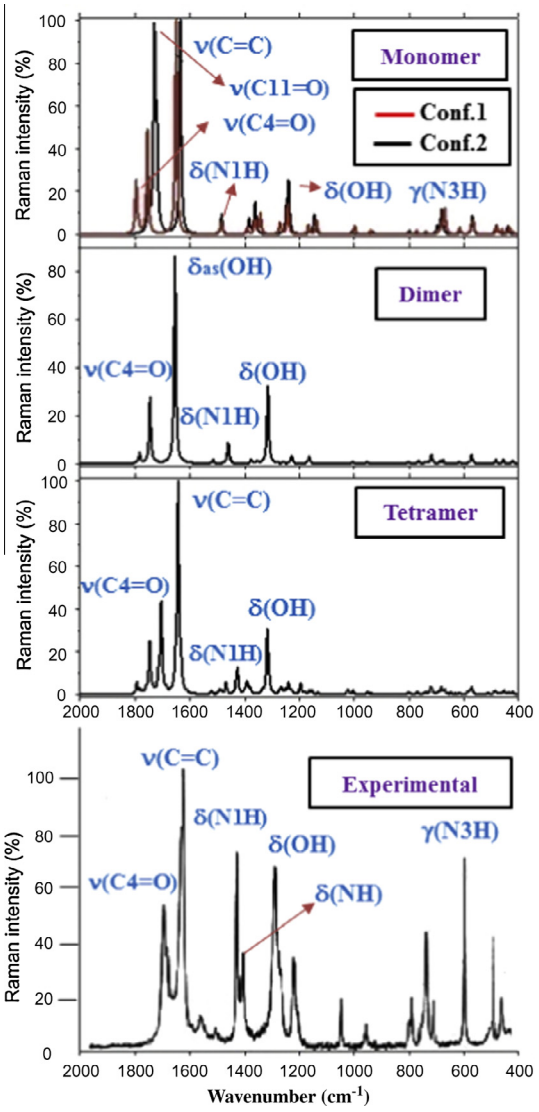

Fig. 8. Theoretical scaled Raman spectrum in the 2000–400 cm^{-1} range of 5-FOA using the scale equation procedure in the monomer, dimer and tetramer simulations, and comparison with the experimental ones.

respectively. They were obtained by normalizing the computed value to the intensity of the strongest band. For comparison purposes, the 2nd column collects the calculated wavenumbers with the 6-31G(d,p) basis set. In column 13th appears the calculated % potential energy distribution (% PED) of the different modes for each computed harmonic wavenumber. Contributions lower than 10% were not considered. The procedure used and developed by us has been described in Refs. [16,17,22]. This characterization of the ring normal modes was compared (12th column) with those found in (U) [22], the first column, using the notation reported for them and numbered from 1 to 30th. A graphical representation of these ring normal modes in 5-FOA is shown in Fig. 9.

Two wavenumbers appear for each vibration corresponding to the two 5-FOA molecules of the dimer, while four wavenumbers appear for the tetramer. Of these four wavenumbers of the tetramer, that with the highest IR intensity is shown in bold type, and its corresponding relative intensity is collected in the column 16th. Analogously, the wavenumber with the highest Raman intensity is printed in Italic type and listed in the column 17th. In each vibration of the tetramer the discussion is mainly centered in the wavenumbers with the highest intensity. It is noted that the highest IR and Raman intensities in the tetramer form correspond to distinct vibrations of those in the isolated state.

The vibrational spectra of 5-FOA are relatively complex. Four contributions of relatively high IR intensity corresponding to carbonyl, carboxylic and amino bending vibrations, are found in the 1300–1700 cm^{-1} wavenumber region. Furthermore, these vibrations appear strongly coupled, and therefore we found it worthwhile to perform a vibrational analysis to assess the usefulness of these vibrations as probes for the bonding situations in their complexes. An analysis of the different vibrations is as follows. The discussion is mainly referred to conformer 2 of 5-FOA.

N—H modes. It has been noted that in general the N—H stretching modes are essentially pure group modes and substitution only induces shifts of about 1%, Table 4. The calculated ν(N1—H) and ν(N3—H) stretching wavenumbers in 5-FOA also appear little affected (something more on N1—H) by the substituent, although their experimental values in the solid state have large differences, due to intermolecular interactions through the H-bonds, Table 6.

In the isolated state, the calculated N1—H stretching vibration is slightly down-shifted at 3587.7 cm^{-1} with the 6-311+G(3df,pd) basis set, as compared to the N3—H stretching vibration (3594.1 cm^{-1}). Similar feature has been observed in orotic acid [24a] with the ν(N3—H) stretching computed at higher wavenumber (3620 cm^{-1}) than the ν(N1—H), 3453 cm^{-1}. This fact observed in both molecules is due to an intramolecular H-contact between H7 and O12 atoms that slightly lengthened the N1—H bond and

Table 4
Comparison of the calculated harmonic wavenumbers (ω, cm^{-1}), relative infrared intensities (A, %), relative Raman scattering activities (S, %), Raman depolarization ratios for plane (P) and unpolarized (UP) incident light, force constants (f, mDyne/Å), and characterization obtained in the isolated state, dimer and tetramer forms of 5-FOA molecule. Comparisons are also with uracil molecule. The highest IR intensity is shown in bold type while the highest Raman intensity is printed in Italic type.

Uracil	isolated state of 5-FOA[a]											Dimer form of 5-FOA[b]		Tetramer form of 5-FOA[b]		
	Anti form							*Syn* form			M[d]	Characterization				
ω[b]	ω[b]	ω	A[c]	S[c]	P	UP	f	ω	A[c]	S[c]			ω	A[c]	ω	A[c]	S[c]
	97	95.1	0	0	0.75	0.86	0.07	98.7	0	0		50% γ(ring) mainly in O10 + 36% γ(C—F) + 14% γ(COOH)	108, 104	0	**123**, *112*, 103, 99	0	0
170	121	120.9	0	0	0.75	0.86	0.09	121.8	0	0	2	75% puckering ring mainly on O8, +15% γ(C—F) + 10% γ(COOH)	141, 126	0	155, 136, *135*, **134**	0	0
150	160	158.8	0	0	0.75	0.86	0.11	156.1	0	0	1	95% puckering on N3	166, 159	6	190, **175**, 173, *164*	0	0
	307	311.8	0	0	0.29	0.44	0.85	304.6	0	0	19[e]	47% δ(C—F) + 25% δ(COO) + 18% δ(C=O in ring)	317, **311**	1	328, **313**, 309, *309*	0	0
	339	341.4	0	2	0.54	0.70	0.89	343.0	0	3		44% δ(C=O in ring) + 28% Δ_s(COO) + 24% δ(C—F)	365, **344**	1	*373*, 357, **353**, 347	0	0
813	360	361.2	0	0	0.75	0.86	0.87	355.6	0	0	13?	61% γ(N1—C6, ring) + 28% γ(C—F)	362, **361**	0	366, 362, **361**, *360*	0	0
385	399	401.3	2	0	0.54	0.70	1.02	410.5	3	1	3	45% δ(ring) + 30% Δ_{as}(COOH) + 25% δ(C—F)	413, 408	2	420, 415, 409, ***406***	0	0
396	449	461.2	0	1	0.75	0.86	0.46	451.0	0	1	4	45% γ(ring) + 26% γ(OH) + 24% γ(C11=O)	477, 470	1	475, 458, 457, ***444***	1	1
519	472	474.0	1	3	0.54	0.70	1.48	470.7	1	3	5	64% δ(ring) + 26% δ(C—F) + 10% Δ_s(COOH)	474, **471**	0	*483*, 479, **477**, 473	1	0
558	564	565.4	0	7	0.13	0.23	1.86	561.8	0	4	7?	78% δ(ring) + 20% Δ_s(COO)	570, **569**	9	**577**, *570*, 568, 565	0	0
563	628	619.3	7	0	0.75	0.86	0.25	613.7	8	2	8	78% γ(N1—H)	619, 618	1	**855**, 634, 612, *585*	2	0
687	682	674.8	3	1	0.75	0.86	0.33	670.4	3	3	9	57% γ(N3—H) + 14% γ(N1—H) + 12% γ(ring) + 10% γ(OH)	**679**, 679	0	**931**, 902, 797, *680*	1	3
541	693	699.7	1	3	0.14	0.25	1.60	690.5	0	1	6	44% Γ(ring) + 18% Δ_{as}(COOH) + 16% δ(C4=O) + 12% δ(C2=O) + 10% δ(C—F)	**694**, 691	0	708, ***701***, 698, 693	1	0
752	739	757.3	5	0	0.75	0.86	2.86	740.0	12	0	11	55% γ(C2=O) + 18% γ(NCN) + 14% γ(N3—H)	739, 739	3	743, **728**, *727*, 727	0	0
729	746	774.9	5	0	0.75	0.86	3.10	744.6	0	1	10	47% γ(N3—C4—C) + 19% γ(C4=O) + 18% γ_s(COOH) + 12% γ(N3—H)	745, **745**	3	747, *746*, 745, **739**	2	0
970	776	805.3	2	1	0.75	0.86	3.82	778.2	5	1	15[e]	50% γ(C6—C11) + 19% γ_s(COO) + 17% γ(C4—C5) + 11% γ(OH)	775, **775**	7	*779*, 776, **776**, 774	0	0
772	810	809.5	6	0	0.70	0.82	2.86	810.7	5	1	12?	45% ν(ring) + 40% ν(C—F)	**815**, 812	0	817, 814, **813**, *809*	5	0
990	956	948.1	0	1	0.33	0.50	3.67	955.2	0	1	16	56% ν(ring) + 21% ν_s(COO) + 13% δ(OH)	970, **970**	0	972, ***969***, 963, 956	0	1
965	1026	1024.9	2	1	0.23	0.38	2.04	1015.6	1	3	14?	46% ν(NCN, ring) + 25% δ(N3—H) + 17% δ(N1—H)	**1030**, 1030	4	1052, *1046*, 1031, **1025**	0	2
	1200	1190.3	10	1	0.42	0.59	3.42	1194.4	4	3		39% ν(ring) + 26% δ(N3—H) + 14% δ(N1—H) + 13% δ(OH)	1197, **1196**	29	1266, **1262**, *1229*, 1214	0	1
1407	1280	1270.1	16	22	0.33	0.50	3.23	1272.7	3	13	21	40% ν(ring) + 26% δ(OH) + 13% ν(C—F) + 12% δ(N1—H)	1264, 1263	7	1304, **1295**, 1288, *1276*	3	0
1198	1293	1277.9	20	9	0.45	0.62	3.23	1302.7	19	5	18	58% ν(C—N, ring) + 26% δ(N1—H)	1296, **1295**		*1358*, **1351**, 1312, 1307	17	3
1382	1415	1401.3	24	3	0.25	0.39	4.26	1399.4	0	5	20	33% ν(C—N3—C) + 16% δ(N3—H) + 16% ν(C—C11) + 15% δ(N1—H) + 13% δ(OH)	1421**, 1420**	40	1446, *1438*, **1435**, 1426	8	4
1506	1429	1421.4	7	7	0.59	0.75	2.83	1429.6	5	3	23	25% δ(N3—H) + 20% δ(N1—H) + 18% ν(NCN) + 12% δ(OH) + 11% ν(C4=O)	1397, 1397	8	1517, **1484**, 1478, *1474*	5	0
3264	1545	1527.2	0	9	0.60	0.75	6.32	1527.7	7	5	28[e]	33% ν(C=C—N1) + 27% ν(C6—C11) + 23% δ(N1—H) + 10% ν(C2=O)	1568, **1558**	0	1574, **1564**, *1544*, 1535	2	0
1690	1708	1686.2	0	100	0.19	0.32	16.68	1702.6	2	97	24?	58% ν(C=C) + 12% δ(N1—H) + 12% ν(C—F) + 10% ν(C11=O)	**1703**, 1690	0	1712, 1703, ***1703***, 1692	1	10
1808	1809	1776.0	100	46	0.29	0.45	16.91	1811.2	59	49	25	61% ν(C4=O) + 14% ν(C2=O) + 11% δ(N3—H) + 10% ν(C11=O)	1811, **1811**	10	1813, 1812, 1778, ***1769***	22	55
1845	1850	1806.4	67	23	0.14	0.26	17.36	1845.9	2	25	26	63% ν(C2=O) + 12% ν(C4=O) + 10% δ(N1—H)	1852, **1850**	0	1850, 1840, *1826*, **1800**	24	2
3658	3607	3587.7	19	39	0.14	0.24	8.17	3647.6	10	57	30	99% ν(N1—H)	**3618**, 3617	0	3637, 3621, 3606, ***3367***	16	83
3620	3616	3594.1	8	6	0.21	0.3	8.20	3615.6	16	40	29	99% ν(N3—H)	3614, **3614**	18	3612, 3505, **3310**, *3273*	49	100

[a] At the B3LYP/6-311++G(3df,pd) level.
[b] At the B3LYP/6-31G(d,p) level.
[c] Normalized to the highest value.
[d] Normal mode of the uracil structure according to Ref. [22]. The question marks indicate a tentative assignment.
[e] Substituent mode in 5-FOA.

Table 5
Scaled wavenumbers (ν, cm^{-1}) obtained with the scale equation procedure from the calculated wavenumbers of Table 4. The values correspond to the uracil ring in the *anti*-form of 5-FOA, in the isolated state and in the dimer and tetramer forms. Comparisons appear with the uracil molecule. The highest IR intensity is shown in bold type while the highest Raman intensity is printed in Italic type. The experimental IR and Raman vibrational wavenumbers are those observed in the solid state. The absolute errors (cm^{-1}) in the scaled wavenumbers of the tetramer are obtained from comparisons with the experimental ones, the underlined values. The characterization is a simplification of that of Table 4.

Uracil		5-FOA									
Isolated state	Exp. gas	Isolated state		Dimer	Tetramer	Experimental		Error[c]		M[d]	Characterization
ν[a]	IR	ν[a]	ν[b]	ν[a]	ν[a]	IR	Raman	(a)	(b)		
		126	124	*136*, **132**	**151**, *140*, 132, 128		141.2 s	17	−10		γ(ring) mainly in O10 + γ(C—F)
195	185	150	147	*168*, **154**	181, 163, *162*, **161**		176.5 s		16	2	puckering ring mainly on O8
176		186	184	*191*, **184**	214, **200**, 198, *190*		217 vw	−7	17	1	puckering on N3
		325	324	*259*, **252**	344, **330**, 326, *326*		326.5 vw	3	−3	19[e]	δ(C—F) + δ(COO) + δ(C=O in ring)
		355	354	334, ***328***	*387*, 372, **368**, 362		388.9 m	35	21		δ(C=O in ring) + Δ_s(COO) + δ(C—F)
803		375	374	*379*, **360**	380, 377, **376**, *375*		375.2 s	1	1	13?	γ(N1—C6, ring) + γ(C—F)
398	374	439	439	**456**, *379*	431, 426, 421, ***418***		420 vw	9	2	3	δ(ring) + Δ_{as}(COOH) + δ(C—F)
409	395	459	459	*425*, **420**	483, 467, 466, ***454***	448 w	449.9 m	−8	−6	4	γ(ring) + γ(OH) + γ(C11=O)
525	512	480	481	*485*, **479**	*491*, 487, **485**, 481	496 m	483.0 m	2	−2	5	δ(ring) + δ(C—F)
562	588	567	568	*573*, **572**	**580**, *573*, 571, 568	587 m	589.3 vs	22	9	7?	δ(ring) + Δ_s(COO)
566	545	628	625	619, *618*	**842**, 635, 613, *587*	875 m			33	8	γ(N1—H)
684	659.5	629	629	***690***, 687	**914**, 887, 788, *677*					9	γ(N3—H)
546	536.4	677	679	**733**, *733*	703, ***697***, 694, 689	713 vw	706.3 m	27	9	6	Γ(ring) + Δ_{as}(COOH)
745	756.5	689	698	**738**, *738*	737, **722**, *721*, 721	732 w	734.5 s	36	12	11	γ(C2=O) + γ(NCN)
723	717.4	733	735	*738*, **738**	**740**, *739*, 738, 733	751 vw	753 sh	18	13	10	γ(N3—C4—C) + γ(C4=O) + γ_s(COOH)
951	972	739	742	*775*, **775**	*770*, 768, **768**, 766		790.2 m	37	22	15[e]	γ(C6—C11) + γ_s(COO)
764	759.2	767	769	**804**, *802*	806, 803, **802,** *798*	805 s	799 sh	181	3	12?	ν(ring) + ν(C—F)
970	990	800	802	*951*, **951**	953, ***950***, 944, 938	950 vw	962.4 vw	159	0	16	ν(ring) + ν_s(COO)
946	952	1005	1009	**1008**, *1008*	1028, *1023*, 1009, **1003**	1058 vw	1057.2 w	56	54	14?	ν(NCN, ring) + δ(N3—H)
		1168	1173	*1165*, **1164**	1231, **1227**, *1196*, 1181			125			ν(ring) + δ(N3—H)
1364	1387	1244	1249	*1259*, **1258**	1266, **1258**, 1241, *1240*	1276 vs 1242 m	1236.9 m	27	18	21	ν(ring) + δ(OH)
1166	1172	1256	1262	*1228*, **1228**	*1317*, **1311**, 1274, 1269	1318 m	1287 sh	28	7	18	ν(C—N, ring) + δ(N1—H)
1340	1356	1371	1378	*1377*, **1376**	1401, *1393*, **1390**, 1382	1378 w			−12	20	δ(N3—H) + ν(C—N3—C)
1457	1461	1384	1391	*1354*, **1354**	1468, **1437**, 1431, *1427*		1449.6 s		13	23	δ(N1—H) + δ(N3—H) + ν(NCN)
3118	3124	1494	1502	*1516*, **1506**	1521, **1512**, *1493*, 1485	1533 w	1528.7 w	−67	17	28[e]	ν(C=C—N1) + ν(C6—C11) + δ(N1—H)
1631	1641	1648	1657	**1643**, *1631*	1652, 1643, ***1643***, 1633	1612 sh	1587.7 w	−69	−31	24?	ν(C=C)
1743	1688	1743	1753	*1745*, **1745**	1747, 1746, 1714, ***1706***	1708 vs	1729.0 s, 1715 m	−18	2	25	ν(C4=O)
1778	1756	1782	1791	*1784*, **1782**	1782, 1773, *1760*, **1735**	1735 vs			0	26	ν(C2=O)
3490	3484	3442	3463	**3452**, *3451*	3470, 3455, 3441, ***3215***	3472 vw, 3169 m		9	−46	30	ν(N1—H)
3454	3436	3451	3471	*3448*, **3448**	3447, 3346, **3162**, *3127*	3513 s, 3108 m		29	−54	29	ν(N3—H)

[a] With the scale equation obtained from uracil molecule [22], $\nu_{scal.} = 34.6 + 0.9447\ \omega_{cal.}$ B3LYP/6-31G(d,p).
[b] With the scale equation obtained from uracil molecule [22], $\nu_{scal.} = 31.9 + 0.9512\ \omega_{cal.}$ B3LYP/6-311++G(3df,pd).
[c] Absolute errors obtained ($\nu_{experimental} - \nu_{scaled}$) in: (a) the calculated wavenumbers of the tetramer, (b) the scaled values of the tetramer using the scale equation procedure.
[d] Ring number according to the notation of Ref. [22]. The question marks indicate a tentative assignment.
[e] Substituent mode in 5-FOA.

Table 6
Comparison of the calculated theoretical harmonic wavenumbers (ω, cm^{-1}), relative infrared intensities (A, %), relative Raman scattering activities (S, %), and Raman depolarization ratios for plane (P) and unpolarized (UP) incident light, reduced masses (μ, AMU) and force constants (f, mDyne/Å) obtained in the carboxylic group of the isolated state, dimer and tetramer forms of 5-FOA. The highest IR intensity is shown in bold type while the highest Raman intensity is printed in Italic type.

Groups	Modes	Isolated state[a]											Dimer[b]		Tetramer[b]		
		Conformer 2 (*anti*)								Conformer 1 (*syn*)							
		ω[b]	ω	A[c]	S[c]	P	UP	μ	f	ω	A[c]	S[c]	ω	A[c]	ω	A[c]	S[c]
COO	ν(C=O)[d]	1813	1784.6	29	92	0.21	0.36	10.45	19.6	1855.9	100	3	**1762**, *1715*	15	1862, *1811*, **1750**, 1670	15	2
	ν(C–O)[e]	1395	1397.7	13	12	0.23	0.38	1.92	2.20	1378.5	31	9	**1355**, 1396	0	1423, 1421, **1397**, *1377*	5	1
	Δ_s[f]	680	682.3	4	9	0.11	0.20	4.47	1.23	681.0	3	3	**750**, *724*	0	753, 721, *686*, **672**	0	0
	Δ_{as}[g]	428	428.8	1	2	0.37	0.53	11.88	1.29	410.5	1	2	*569*, **569**	0	**505**, 468, *441*, 425	0	1
	Γ[h]	183	182.2	0	0	0.67	0.80	9.56	0.19	180.3	0	0	**230**, *166*	0	***249***, 230, 193, 185	0	0
	τ[i]	97	59.8	0	0	0.75	0.86	12.37	0.03	55.4	0	0	**125**, *103*	0	**106**, 98, *80*, 71	0	0
OH	ν	3754	3744.0	14	98	0.27	0.42	1.06	8.79	3760.0	14	100	**3150**, *3034*	100	3767, 3730, **3173**, *3060*	100	5
	δ[j]	1184	1171.3	16	8	0.18	0.30	3.02	2.44	1363.3	53	5	*1264*, **1263**	0	1517, **1484,** *1358*, 1351	5	0
	γ[k]	629	609.9	10	1	0.75	0.86	1.30	0.28	568.7	16	3	**989**, *947*	4	**975**, 923, *649*, 619	3	0

[a] At the B3LYP/6-311++G(3df,pd) level.
[b] At the B3LYP/6-31G(d,p) level.
[c] Normalized to the highest value.
[d] +ν(C4=O) + δ(ring).
[e] +δ(N3–H) + δ(OH) + δ(N1–H).
[f] +δ(ring).
[g] +δ(ring).
[h] +δ(C–F) + δ(ring).
[i] +τ(ring).
[j] +ν(C–O) + δ(N1–H).
[k] +γ(N1–H) + γ(N3–H).

consequently decrease its stretching wavenumber. It is worthwhile to note that in the *syn* form of 5-FOA both N–H stretching vibrations appear at higher wavenumbers as compared to *anti*-form due to the absence of H-contacts.

In the case of 5-aminoorotic acid, the very weak experimental Raman band observed at 3456 cm^{-1} (3457 cm^{-1} by IR) was erroneously assigned [26c,d] to the ν(N3–H) mode instead of the ν(N1–H) mode. It was due to the calculated wavenumber by Kostova et al. [26c,d] by B3LYP at 3583 cm^{-1} was not scaled.

The experimental band detected at 3169 cm^{-1} was assigned to the N1–H stretch, and related to the scaled value at 3215 cm^{-1} in our tetramer simulation, Table 5. The very weak band registered at 3472 cm^{-1} can also be assigned to the N1–H stretching mode, but only in molecules which are not associated through H-bonds to this group, in accordance to the scaled value at 3452 cm^{-1} obtained in the dimer, and to the value of 3442 cm^{-1} found in the isolated state.

In the tetramer model of 5-FOA the N3–H moiety has intermolecular H-bonds with adjacent molecules which produce a lowering ca. 300 cm^{-1} of its stretching mode. Thus, in the isolated state the ν(N3–H) wavenumber is scaled at 3451 cm^{-1} (3rd column of Table 5), similar to that calculated in the dimer at 3448 cm^{-1}, but in the tetramer it appears scaled at 3162 cm^{-1} (with the highest IR intensity) and closed to the experimental IR band at 3108 cm^{-1}. The difference between scaled-experimental indicate that in the crystal, due to the interactions of our tetramer with adjacent ones, the intermolecular H-bonds are relaxed and as consequence the N3–H bond is slightly larger in our calculations. The strong and broad band detected at 3513 cm^{-1} can be related to molecules that are not H-bonded to this group.

In the in-plane N–H bending modes the main contributions correspond to mode no. **23**, δ(N1–H, N3–H) and no. **20**, δ(N3–H), where the numbers 23 and 20 refer to the ring normal modes no. 23 and 20, respectively of uracil molecule [22]. These modes appear strongly coupled with ν(C–N) modes. They appear scaled in the isolated state at 1384 and 1371 cm^{-1}, respectively, 1437 and 1390 cm^{-1} by IR (1427 and 1393 cm^{-1} by Raman), respectively, in the tetramer. A good accordance was obtained with the corresponding experimental bands. All the vibrations in the 1500–1000 cm^{-1} range have, in general, significant contributions of these δ(N–H) modes.

In the out-of-plane N–H bending modes γ(N–H), the γ(N3–H) mode (no. **9**) is predicted to occur in the isolated state at 629 cm^{-1}. In the tetramer form this mode changes to remarkably higher wavenumbers up to 900 cm^{-1}. Thus, it is scaled at 914 cm^{-1} with weak IR and Raman intensities, but the bands were not detected in the experimental spectra. The γ(N1–H) mode (no. **8**) is predicted in the isolated state at 628 cm^{-1} with medium IR intensity, but in the tetramer form it raised up to 842 cm^{-1} with weak IR intensity and almost null Raman activity in great accordance with its not detection in the experimental spectra. The IR band observed at 875 cm^{-1} was assigned to this mode.

C=O ring modes. The double bond (C=O and C=C) stretching regions are known to be very sensitive. The C=O modes are very important because the C=O groups take part in hydrogen bonding, especially in nucleic acid base derivatives [11,12a]. Therefore, comparison of C=O stretching wavenumbers in different nucleic acid base derivatives has been reported [12b,c]. In the isolated state, two very strong IR bands appear scaled at 1791 and 1753 cm^{-1}, corresponding to ν(C2=O) and ν(C4=O) modes, respectively, and coupled significantly with other stretching and bending modes. Due to the H-bonds formation of the tetramer form their scaled wavenumbers appear at slightly lower values than in the isolated state, at 1735 and 1706 cm^{-1}, respectively, and in better accordance with the experimental bands observed in the solid state with very strong IR intensity at 1735 and 1708 cm^{-1}. In the Raman spectrum three bands are observed at 1729.0, 1715 and 1658.6 cm^{-1} corresponding to the C=O stretching. The first two are assigned to the C4=O group in accordance to its scaled wavenumber by Raman at 1706 cm^{-1} and to its very strong Raman intensity predicted, while the last one is assigned to the COO group in accordance to the Raman band predicted at 1675 cm^{-1}.

Compared to (U), it is observed that in 5-FOA the calculated ν(C2=O) bands position remains almost unaffected by changes in the molecular structure of the uracil ring [22]. Thus, it is calculated at 1850 cm^{-1} in 5-FOA vs. 1845 cm^{-1} in uracil at the B3LYP/6-31G(d,p) level. This is caused by the fact that the C2=O group is

Table 7
Scaled and experimental vibrational wavenumbers (in cm^{-1}) of the carboxylic group in conformer 2 of 5-FOA and at the B3LYP/6-31G(d,p) level. The experimental underlined values correspond to those selected for comparison with the theoretical ones.

Groups	Modes	Isolated State			Dimer	Tetramer	Experimental		Errors[d]			
		ν[a]	Factor[b]	ν[c]	ν[a]	ν[a]	IR	Raman	(a)	(b)	(c)	(d)
COO	ν(C═O)	1734	0.9632	1746	**1686**, *1642*	1809, *1732*, **1675**, 1599	1676 vs	1658.6 vs	−137	−58	−70	1
	ν(C—O)	1339	0.9677	1338	***1301***, 1334	1365, 1363, **1341**, *1322*		1307.4 vs	−88	−32	−31	−34
	Δ_s	662	1.0078	685	**728**, *703*	739, 701, *670*, **654**						
	Δ_{as}	423	0.8843	378	*557*, **557**	**497**, 461, *436*, 420						
	Γ	192	0.9125	167	**236**, *157*	***254***, 236, 201, 193		252.6 w	70	61	86	17
	τ	111	1.3303	129	**137**, *116*	**119**, 111, *94*, 86		90.4 vs	−7	−21	−39	−47
OH	ν	3570	0.9479	3558	**2999**, *2900*	3583, 3548, **3021**, *2914*	3014 m	3003.3 w	−770	−586	−574	−37
	δ	1296	0.9598	1295	*1216*, **1214**	1454, **1423**, *1303*, 1297	1435 vs	1431.9 m	248	136	137	12
	γ	623	1.0346	650	**955**, *915*	**941**, 892, *633*, 604	961 m		321	327	300	9

[a] With the scaling equation from benzoic acid [30], $\nu_{exp.} = 18.8 + 0.9462 \cdot \omega_{cal.}$
[b] Specific scale factors from benzoic acid [30].
[c] With the specific scale factors of the previous column.
[d] Errors obtained ($\nu_{experimental} - \nu_{scaled}$) in the wavenumbers: (a) calculated in the isolated state, (b) scaled with the scale equation in the isolated state, (c) scaled with specific scale factors in the isolated state, (d) scaled with the scaled equation in the tetramer.

quite distanced from the —COOH and —F groups and, moreover, it is surrounded by the two N—H groups, which buffer it from influences of the remaining molecular moieties. On the other hand, the C4═O moiety is nearer to the F atom and it also buffer the influence on the other atoms.

The C2═O and C4═O in-plane bending modes appear strongly coupled with ring modes and spread out in different vibrations. Thus, they were included in the ν(ring) characterization, Table 4.

The out-of-plane bending modes are also strongly coupled with ring modes. The γ(C4═O) mode (no. **10**) is predicted in the tetramer at 740 cm^{-1} with medium IR intensity and null Raman activity, in accordance with the very weak experimental IR band at 751 cm^{-1} and Raman line at 753 cm^{-1}. The γ(C2═O) mode (no. **11**) is scaled in the isolated state at 698 cm^{-1} and in the tetramer form at 722 cm^{-1} in good accordance with the experimental bands at 732 cm^{-1} (IR) and 734.5 cm^{-1} (Raman).

C—C and C—N ring modes. It has been observed that the C═C stretching vibration (no. **24**), scaled in the isolated state at 1657 cm^{-1}, appears coupled with the δ(N1—H), ν(C—F) and ν(C11═O) modes, in contrast to that observed in 5-A.U. [10], where the ν(C═C) vibration appears only coupled with the δ(N—H) and δ(C6—H) modes. The coupling in 5-FOA makes difficult the clear characterization of the motions corresponding to this vibration no. 24. In the tetramer it is predicted with very weak IR intensity at 1643 cm^{-1}, in accordance with the shoulder observed at 1612 cm^{-1} in the experimental IR spectrum. The Raman band is predicted with high intensity, one of the highest in the middle-IR region, and related to the experimental Raman band at 1587.7 cm^{-1}. An increase in the ν(C═C) wavenumber appears related [11,12] to an increment in the negative charge on substituent (F) in position 5.

Ring modes vibrations also correspond to nos. **28, 18, 21, 14, 16** and **12**. They appear strongly coupled with other stretch and bend modes. Mode no. **18** is mainly characterized as a ν(C—N) stretch and it is predicted in the tetramer with strong IR intensity at 1311 cm^{-1} in good accordance to the experimental band with medium intensity at 1318 cm^{-1}. The wavenumber of the ν(C—N) modes is slightly higher in the tetramer form as compared to that in the isolated state. Mode **14** is predicted with weak Raman intensity at 1023 cm^{-1} and it was related to the Raman line at 1057.2 cm^{-1}.

Mode **12** appears strongly coupled with the C—F stretch, which makes its characterization difficult. It is predicted with medium IR intensity at 802 cm^{-1} in the tetramer form in excellent accordance to the strong band observed at 805 cm^{-1}. This mode is predicted with almost null Raman intensity at 798 cm^{-1}, also in good accordance to the shoulder detected at 799 cm^{-1}.

The out-of-ring vibrations correspond to modes **4, 13, 1** and **2**. Also the calculated vibration at 95.1 cm^{-1} is an out-of-ring vibration but we cannot identify it as an uracil ring mode. They are predicted with very weak or almost null IR and Raman intensity and strongly coupled with other out-of-plane modes. Their scaled wavenumbers in the isolated state differ little of those in the tetramer. The puckering on N3 and N1 is calculated with the 6-31G(d,p) basis set at 160 and 121 cm^{-1}, respectively, while in uracil molecule they were calculated at 150 and 170 cm^{-1}, respectively. It means that the —F and —COOH substituents remarkably reduce the wavenumber on the puckering on N1, and they have little effect on N3.

C—F modes. The C—F group gives rise to its stretching wavenumber in the region 1000–1450 cm^{-1} and usually appears with strong intensity in both Raman and infrared spectra. In the present study C—F stretch appears distributed mainly in several modes, no. **24, 21** and **12.** In the last one, the contribution reaches the 40%.

The in-plane δ(C—F) bending is also distributed in several modes, no. 6, 5, 3 and 19, and as well in the Γ(COO) mode calculated at 183 cm^{-1} in the isolated state. The main contribution corresponds to mode **19,** a substituent mode, strongly coupled with COO, C2═O and C4═O bendings, and predicted with very weak Raman intensity at 326 cm^{-1}, in excellent agreement with the Raman line at 326.5 cm^{-1}.

The out-of-plane γ(C—F) bending appears at wavenumber lower than 400 cm^{-1}. It is predicted with very low and almost null IR and Raman intensity, but we have detected them in the Raman lines with strong intensity at 375.2, 176.5 and 141.2 cm^{-1}. An excellent accordance is found in our scaled values in the tetramer at 375, 162, and 140 cm^{-1}.

COOH group vibrations

O—H modes. In Table 6 is shown the calculated harmonic wavenumbers obtained for the different modes of the carboxylic group, while the scaled and experimental wavenumbers using the scaling procedures mentioned above were included in Table 7.

The stretching ν(O—H) is characterized as a pure mode at 3570 cm^{-1} in the isolated state with the scaling equation procedure. Its wavenumber drops up to 3021 cm^{-1} in the tetramer form and it appears with the highest IR intensity. This mode was assigned to the observed IR band at 3014 cm^{-1}. The shoulder detected at 2921 cm^{-1} can correspond also to ν(O—H) but in molecules with strong intermolecular H-bonds. The weak band at 3619 cm^{-1} can be also assigned to the O—H stretching but in molecules which are not associated through this group.

The very strong IR band at 1435 cm^{-1} was assigned to the in-plane bending, δ(OH) in accordance to the scaled value in the

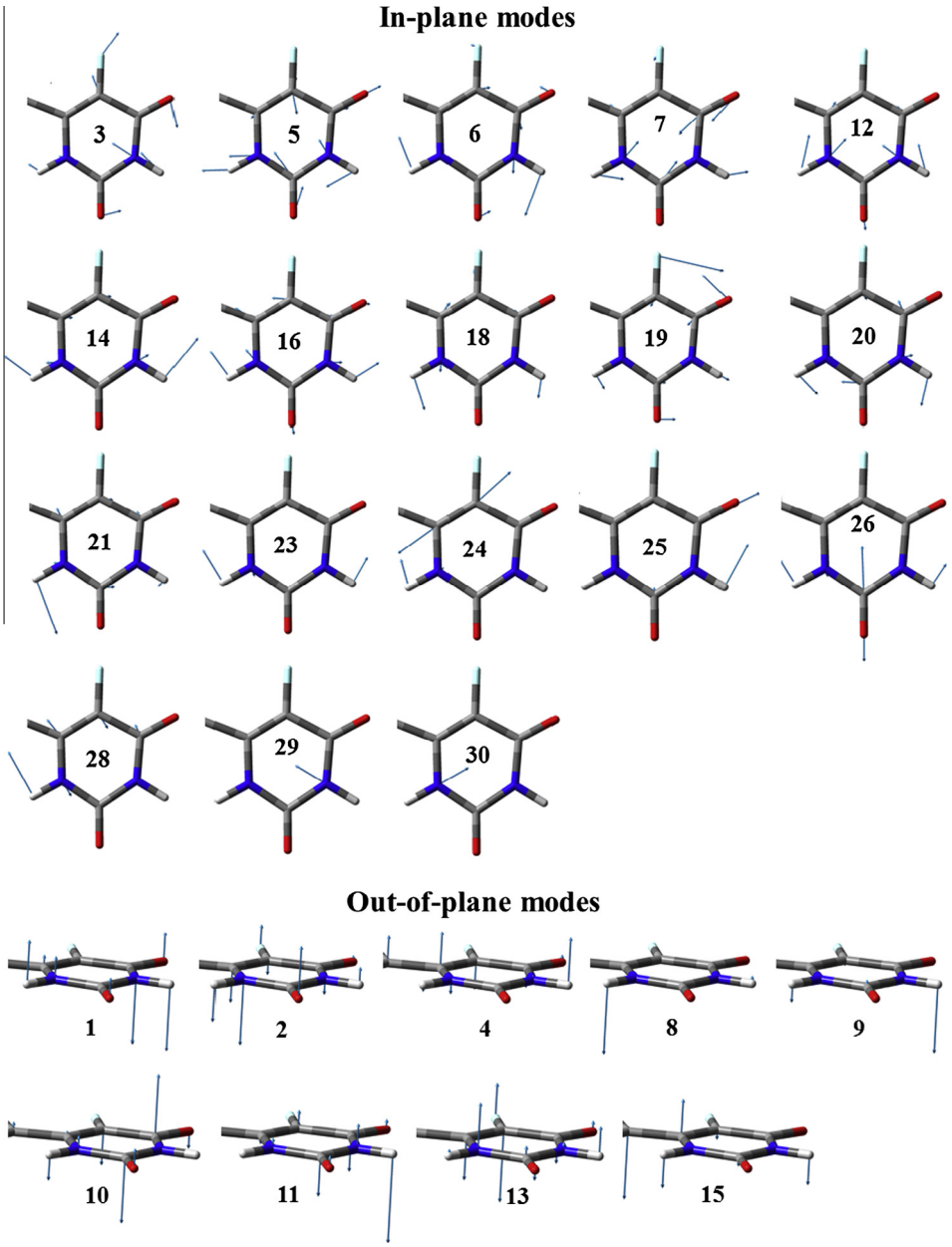

Fig. 9. A graphical representation at the B3LYP/6-31G(d,p) level of the ring normal modes in 5-FOA.

tetramer form at 1423 cm^{-1}. The corresponding Raman band was detected at 1431.9 cm^{-1}. This mode appears strongly coupled with ν(COO) and δ(N1—H) modes. Also, different contributions of this mode appear spread out in the scaled wavenumbers at 1391, 1378, 1249, 1173 and 802 cm^{-1} of the isolated state. Due to this coupling and the different % contribution in the distinct calculated wavenumbers, it was reported at 1139 cm^{-1} in benzoic acid [30] and at 1149 cm^{-1} in 5-aminoorotic acid [9].

γ(O—H) modes are in general characterized as almost pure modes. In 5-FOA appears weakly coupled with the τ(ring) torsional mode. Its scaled wavenumber in the tetramer at 941 cm^{-1} with medium IR intensity is in good accordance to the band observed at 961 cm^{-1}. A significant contribution of this mode also appears in the normal mode **4**.

COO modes. The very strong IR band at 1676 cm^{-1} was assigned to the ν(C═O) mode of the carboxylic group. In 5-aminoorotic acid [9] the strong band at 1667 cm^{-1} was assigned to this mode.

The in-plane bending modes, denoted as Δ_s(COO), Δ_{as}(COO) and Γ(COO) appear strongly coupled with ring modes and spread out in different vibrations. The modes corresponding to the —COO group appear predicted with very weak or almost null IR and Raman intensity in the tetramer form at 654, 497 and 254 cm^{-1}, respectively, in accordance to its no detection in the experimental spectra. Only a weak Raman line at 252.6 cm^{-1} was observed and assigned to the rocking Γ(COO) mode.

The torsional τ(COO) mode was scaled at 119 cm^{-1} in IR and 94 cm^{-1} in Raman, in accordance to the Raman band at 90.4 cm^{-1}. In 5-aminoorotic acid it was predicted at 150 cm^{-1}. The significant difference in the wavenumber is due to the distinct effect of the —NH_2 and —F substituents on the COO modes.

The experimental bands detected at 2847 and 2477 cm^{-1} (IR) and 2836.5 cm^{-1} (Raman) can be assigned to overtones or combination bands.

Table 8
Calculated low vibrational modes at the B3LYP/6-31G(d,p) level in the dimer and tetramer forms of conformer 2 in 5-FOA. The frequencies with question marks are tentative.

Characterization	Dimer	Tetramer
δ (H-bond stretching)	92	117, 65, 63
δ (H-bond shearing)	83	83, 57, 52
γ (tilting "slanting")	55	62?, 41, 33?
δ (cogwheel)	43	48, 44, 22
γ (torsion "twist")	17	16, 14?, 12
γ (butterfly)	16	20, 9?, 6

Lattice modes

The low vibrational modes calculated in the dimer and tetramer forms of 5-FOA are collected in Table 8. The notation used in the characterization of the modes is in accordance to that reported in other molecules [30,32]. For each mode, those vibrations which appear with the highest IR intensity are printed in bold type. A graphical description of these modes is plotted in Fig. 10 for the dimer form.

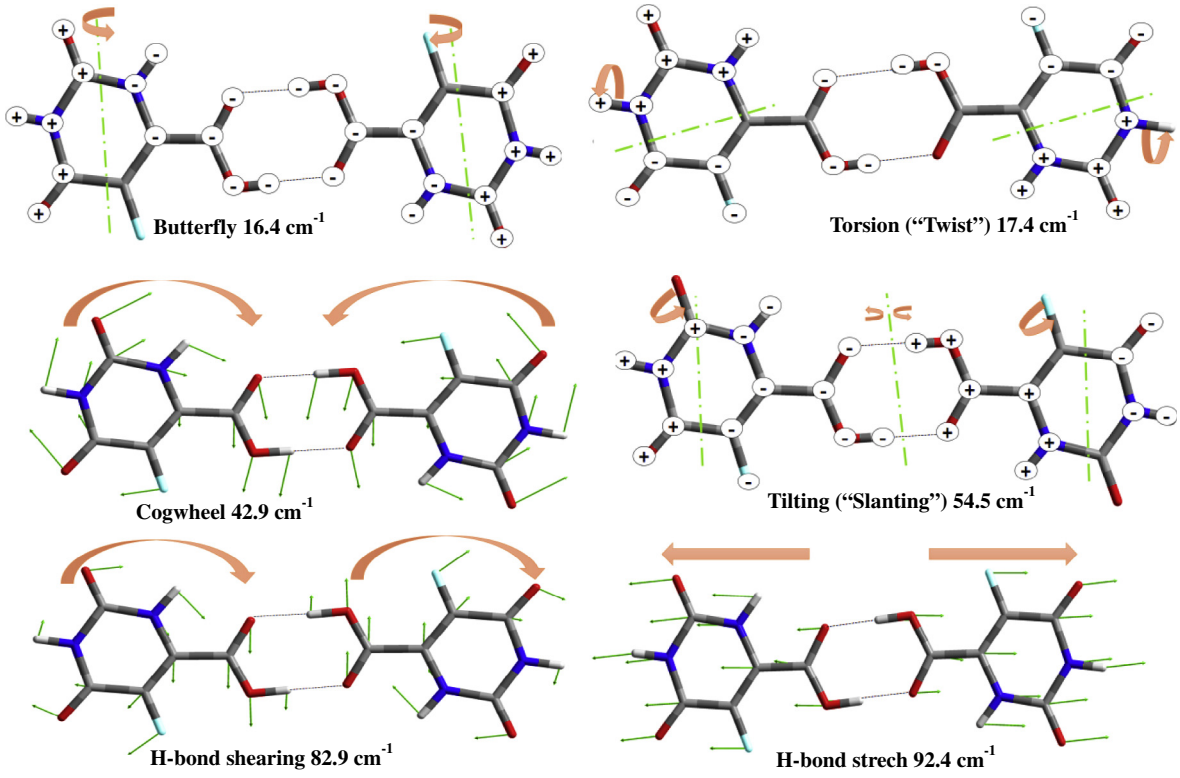

Fig. 10. Characteristic skeletal modes in the low wavenumber range (<100 cm^{-1}) calculated in the dimer form of conformer 2 of 5-FOA at the B3LYP/6-31G(d,p) level. The wavenumber and the description shown correspond to that with higher IR intensity.

Table 9
Theoretical computed total energies (A.U.[#]), zero-point vibrational energies (kJ mol^{-1}), rotational constants (GHz), entropies (J mol^{-1} K^{-1}) and dipole moments (D) calculated at different levels in the two conformers of the isolated state of 5-FOA, and in its dimer and tetramer forms.

Parameters	Conformer 1 (*syn*)			Conformer 2 (*anti*)			Dimer	Tetramer
	B3LYP/ 6-31G(d,p)	B3LYP/ 6-311++G(3df,pd)	MP2/ 6-31G(d,p)	B3LYP/ 6-31G(d,p)	B3LYP/ 6-311++G(3df,pd)	MP2/ 6-31G(d,p)	B3LYP/ 6-31G(d,p)	B3LYP/ 6-31G(d,p)
ΔE + ZPE	.519100[a]	.782794	.756052[b]	.522408[a]	.786012[a]	.758909[b]	.072198[c]	.145789[d]
Zero-point energy	245.9	245.9		246.5	245.3		496.0	994.1
ΔG	.555261[a]	.818954[a]		.558376[a]	.822069[a]		.125852[c]	.235880[d]
Rotational constants	1.284	1.284	1.279	1.293	1.306	1.287	0.632	0.072
	0.872	0.872	0.874	0.870	0.874	0.873	0.074	0.020
	0.519	0.520	0.519	0.520	0.524	0.520	0.066	0.016
Entropy								
Total	414.4	414.4		411.9	412.7		667.1	1195.8
Translational	173.1	173.1		173.1	173.1		181.7	190.4
Rotational	128.4	128.4		128.4	128.3		150.2	170.4
Vibrational	112.8	112.9		110.5	111.3		335.2	835.0
Dipole moment	3.185	3.814	3.273	3.034	3.057	4.243	0.297	4.725

[#] 1 A.U. = 2627.256 kJ mol^{-1}.
[a] −702.
[b] −700 (without ZPE correction).
[c] −1405.
[d] −2810.

Other molecular properties

As in our previous publications [12a,12b,12c], the calculated wavenumbers have been employed to yield thermodynamic properties, such as enthalpy, heat capacity, free energy and entropy, which are collected in Table 9. The theoretical data are employed to correct experimental thermochemical information at 0 K, and as well as for the effect of the zero-point vibrational energy (ZPVE). For the ZPVE, scaling factors can be used [17] to improve their overestimation.

To observe the convergence of the energy and thus to analyze the quality of the theoretical results, several basis sets were used. A small increase of energy was observed with the increment of the 6-311++G(3df,pd) basis. Therefore the results obtained in the table with this basis can be considered acceptable. Several thermodynamic parameters such as enthalpy, heat capacity, free energy and entropy have been calculated in 5-FOA. Small differences in the parameters were observed with the increase of the basis set. The differences have been attributed to the neglect of residual (orientation) entropy present at 0 K in the crystal.

The two possible locations for the carboxylic proton give rise to significantly different dipole moments for conformer *anti* (3.05 D) and for conformer *syn* (3.81 D) with the 6-311++G(3df,pd) basis set. It means that *syn*-form increases its stability in water solution as compared to *anti*-form. The calculated value of dipole moment in 5-FOA is slightly lower than in (U), as well as in other uracil derivatives.

Summary and conclusions

In the present work we have carried out a structural, tautomeric and spectroscopic study of the 5-fluorootic acid by DFT and MP2 methods. The main conclusions of this research are the following:

(1) Energies obtained by B3LYP and MP2 methods and with different basis sets indicated that although the energy difference between *anti*- and *syn*-forms is small, *anti*-form is the most stable one.
(2) Considering the *anti*-form, all the tautomers were studied. Each tautomer has two different possibilities according to the spatial arrangement of the hydrogen atoms, which migrates to give a total of 11 tautomers. The most stable one corresponds to the *keto* T1 form. The *enols* T2b and T3b are the 2nd and 3rd most stable with close energies between them, and more stable than the remaining tautomers.
(3) The —F substituent has higher effect on the uracil ring charges than the —COOH substituent. The negative charge in C5 atom passes to positive value in 5-FOA, while the positive value in C6 atom is significantly reduced.
(4) In the spectroscopic study, the FT-IR and FT-Raman experimental spectra were compared mainly with the simulated spectra of the isolated state and tetrameric structures. The harmonic wavenumbers have been determined and the values analyzed. The results obtained appear as the most accurate today.
(5) To improve the calculated harmonic wavenumbers the linear scaling equation procedure was used. These results appear very accurate with errors less than 5%. The difference between the observed and scaled wavenumber values of most of the fundamentals is in general very small, and therefore the assignments seem to be correct. Bands that did not appear in our computed spectra were not observed in the experimental one, which further confirms our simulations.
(6) In the simulation with a dimer and a tetramer form, the scaled wavenumbers are in better accordance with the experimental IR and Raman data in the solid state than in the isolated form. In these dimeric and tetrameric forms, the bands due to OH and NH groups appear at lower wavenumbers, because the hydrogen bonds formed cause a weakening of the OH and NH bonds.

Acknowledgements

V.K.R. is thankful to Sri Rakesh Mohan Garg, Chairman and Dr. Diasy Bhat, Director, R.D. Foundation Group of Institutions, Kadrabad (Modinagar), Ghaziabad, India for encouragement and providing computer facility during the final submission of this paper. V.K.R. is also grateful to Sri V.C. Goel, Vice Chancellor, CCS University, Meerut for motivation and encouragement during the first draft of the manuscript, when he was in CCS University, Meerut.

Appendix A. Supplementary material

Supplementary data associated with this article can be found, in the online version, at http://dx.doi.org/10.1016/j.saa.2014.04.107.

References

[1] (a) R. Hilal, Z.M. Zaky, S.A.K. Elroby, J. Mol. Struct. (Theochem) 685 (2004) 35–42;
(b) K. Helios, M. Duczmal, A. Pietraszko, D. Michalska, Polyhedron 49 (2013) 259–268;
(c) F.L. Rosenfeldt, Cardiovasc. Drugs Ther. 12 (1998) 147;
(d) H. Van der Meersch, J. Pharm. Belg. 4 (2006) 97;
(e) O. Kumberger, J. Riede, H. Schmidbaur, Z. Naturforsch. B48 (1993) 961.
[2] M. Wellington, E. Rustchenko, Yeast 22 (2005) 57–70.
[3] A.G. Schneider, H.W. Schmalle, F. Arod, E. Dubler, J. Inorg. Biochem. 89 (2002) 227–236.
[4] R. Kareen, H.M. Kieler-Ferguson, J. Katherine, F.C. Szoka Jr., J. Controlled Release 153 (2011) 288–296.
[5] J.D. Boeke, J. Trueheart, G. Natsoulis, G. Fink, Methods Enzymol. 154 (1987) 164–175.
[6] F.W. Muregi, I. Ohta, U. Masato, H. Kino, A. Ishih, PLoS One 6 (6) (2011) e21251, 1–12.
[7] T. Yano, C. Sanders, J. Catalano, F. Daldal, Appl. Environ. Microb. 71 (2005) 3014–3024.
[8] N. Ko, R. Nishihama, J.R. Pringle, Yeast 25 (2008) 155–160.
[9] S. Ortiz, M. Alcolea Palafox, V.K. Rastogi, R. Tomer, Spectrochim. Acta A 97 (2012) 948–962.
[10] M. Alcolea Palafox, G. Tardajos, A. Guerrero-Martínez, V.K. Rastogi, D. Mishra, S.P. Ojha, W. Kiefer, Chem. Phys. 340 (2007) 17–31.
[11] M. Alcolea Palafox, O.F. Nielsen, K. Lang, P. Garg, V.K. Rastogi, Asian Chem. Lett. 8 (1) (2004) 81–93.
[12] (a) M. Alcolea Palafox, G. Tardajos, A. Guerrero-Martínez, J.K. Vats, H. Joe, V.K. Rastogi, Spectrochim. Acta A 75 (2010) 1261–1269;
(b) V. K Rastogi, M. Alcolea Palafox, A. Guerrero-Martinez, G. Tardajos, J.K. Vats, I. Kostova, S. Schlucker, W. Kiefer, J. Mol. Struct. (Theochem) 940 (2010) 29–44;
(c) M. Alcolea Palafox, V.K. Rastogi, A. Guerrero-Martínez, G. Tardajos, H. Joe, J.K. Vats, Vib. Spectrosc. 52 (2010) 108–121;
(d) M. Alcolea Palafox, V.K. Rastogi, H. Kumar, I. Kostova, J.K. Vats, Spectrosc. Lett. 44 (2011) 300–306;
(e) S. Ortiz, M.C. Alvarez-Ros, M. Alcolea Palafox, V.K. Rastogi, V. Balachandran, S. Rathod, Spectrochim. Acta. (in press), http://dx.doi.org/10.1016/j.saa.2014.04.009.;
(f) H.P. Mital, S. Bhardwaj, S.K. Singhal, R.K. Sharma, Asian Chem. Lett. 1 (1999) 77.
[13] J.M. Seminario, P. Politzer (Eds.), Theoretical and Computational Chemistry: Modern Density Functional Theory: A Tool for Chemistry, vol. 2, Elsevier, Amsterdam, 1995.
[14] A.D. Becke, J. Chem. Phys. 98 (1993) 5648.
[15] C. Lee, W. Yang, R.G. Parr, Phys. Rev. B 37 (1988) 785.
[16] M. Alcolea Palafox, Int. J. Quant. Chem. 77 (2000) 661–684.
[17] M. Alcolea Palafox, Recent Res. Dev. Phys. Chem. 2 (1998) 213–232.
[18] M. Alcolea Palafox, N. Iza, M. Gil, V.K. Rastogi, in: Kehar Singh, V.K. Rastogi (Eds.), Perspectives in Engineering Optics, Anita Pub., Delhi, India, 2002, pp. 356–391.
[19] M. Alcolea Palafox, V.K. Rastogi, R.P. Tanwar, L. Mittal, Spectrochim. Acta A 59 (2003) 2473–2486.

[20] (a) M. Alcolea Palafox, V.K. Rastogi, Spectrochim. Acta A 58 (2002) 411–440;
(b) M. Alcolea Palafox, J. Talaya, A. Guerrero-Martinez, G. Tardajos, H. Kumar, J.K. Vats, V.K. Rastogi, Spectrosc. Lett. 43 (2010) 51–59.
[21] M.J. Frisch, G.W. Trucks, H.B. Schlegel, G.E. Scuseria, M.A. Robb, J.R. Cheeseman, J.A. Montgomery Jr., T. Vreven, K.N. Kudin, J.C. Burant, J.M. Millam, S.S. Iyengar, J. Tomasi, V. Barone, B. Mennucci, M. Cossi, G. Scalmani, N. Rega, G.A. Petersson, H. Nakatsuji, M. Hada, M. Ehara, K. Toyota, R. Fukuda, J. Hasegawa, M. Ishida, T. Nakajima, Y. Honda, O. Kitao, H. Nakai, M. Klene, X. Li, E. Knox, H.P. Hratchian, J.B. Cross, C. Adamo, J. Jaramillo, R. Gomperts, R.E. Stratmann, O. Yazyev, A.J. Austin, R. Cammi, C. Pomelli, J.W. Ochterski, P.Y. Ayala, K. Morokuma, G.A.Voth, P. Salvador, J.J. Dannenberg, V.G. Zakrzewski, S. Dapprich, A.D. Daniels, M.C. Strain, O. Farkas, D.K. Malick, A.D. Rabuck, K. Raghavachari, J.B. Foresman, J.V. Ortiz, Q. Cui, A.G. Baboul, S. Clifford, J. Cioslowski, B.B. Stefanov, G. Liu, A. Liashenko, P. Piskorz, I. Komaromi, R.L. Martin, D.J. Fox, T. Keith, M.A. Al-Laham, C.Y. Peng, A. Nanayakkara, M. Challacombe, P.M.W. Gill, B. Johnson, W. Chen, M.W. Wong, C. Gonzalez, J.A. Pople, Gaussian 03, Revision B.04 Inc., Pittsburgh PA, 2003.
[22] M. Alcolea Palafox, N. Iza, M. Gil, J. Mol. Struct. (Theochem) 585 (2002) 69–92.
[23] J.E. Carpenter, F. Weinhold, J. Mol. Struct. (Theochem) 169 (1988) 41.
[24] (a) G. Portalone, Acta Crystallogr. E 64 (2008) o656;
(b) L. Guidoni, L. Gontrani, L. Bencivenni, C. Sadun, P. Ballirano, J. Phys. Chem. A 113 (2009) 353.
[25] S. Bekiroglu, O. Kristiansson, J. Chem. Soc. Dalton Trans. 7 (2002) 1330.
[26] (a) V.K. Rastogi, V. Jain, R.A. Yadav, C. Singh, M. Alcolea Palafox, J. Raman Spectrosc. 31 (2000) 595–603;
(b) M. Alcolea Palafox, V.K. Rastogi, H. Kumar, I. Kostova, J.K. Vats, Spectrochim. Acta A 79 (2011) 970–977;
(c) I. Kostova, N. Peica, W. Kiefer, J. Raman Spectrosc. 38 (2007) 205;
(d) I. Kostova, N. Peica, W. Kiefer, Chem. Phys. 327 (2006) 494.
[27] S. Frean, M. Alcolea Palafox, V.K. Rastogi, J. Mol. Struct. 1054–1055 (2013) 32–45.
[28] M. Alcolea Palafox, J.L. Núñez, M. Gil, J. Mol. Struct. (Theochem) 593 (2002) 101–131.
[29] M. Alcolea Palafox, M. Gil, J.L. Núñez, V.K. Rastogi, L. Mittal, R. Sharma, Int. J. Quant. Chem. 103 (4) (2005) 394–421.
[30] M. Alcolea Palafox, J.L. Núñez, M. Gil, Int. J. Quant. Chem. 89 (2002) 1–24.
[31] C. Singh, M. Alcolea Palafox, N.P. Bali, S.S. Bagchi, P.K. Shrivastava, Asian Chem. Lett. 3 (3) (1999) 248–249.
[32] M. Alcolea Palafox, V.K. Rastogi, Satendra Kumar, H. Joe, Spectrochim. Acta A 111 (2013) 104–122.